International Journal of Pharmaceutics

Development of flexible nanocarriers for siRNA delivery into tumor tissue

Hyunkyung Jung[1], Yuri Shimatani[1], Mahadi Hasan[1], Kohei Uno[1], Susumu Hama[1], Kentaro Kogure[2]*

[1]Kyoto Pharmaceutical University, Misasagi-Nakauchicho 5, Yamashina-ku, Kyoto 607-8414, Japan

[2]Department of Pharmaceutical Health Chemistry, Tokushima University Graduate School of Biomedical Sciences, Shomachi 1, Tokushima, 770-8505, Japan

*Correspondence should be addressed to Kentaro Kogure, Ph. D.

Department of Pharmaceutical Health Chemistry,

Tokushima University Graduate School of Biomedical Sciences

Shomachi 1, Tokushima, 770-8505, Japan

Tel.: +81-88-633-7248, Fax: +81-88-633-9572

E-mail: kogure@tokushima-u.ac.jp

Abstract

Various non-viral delivery systems for small interfering RNAs (siRNA) have been developed. Such delivery systems generally exhibit tightly formed spherical structures. While such carriers have demonstrated good transfection activity in mono-layered cell systems, effects against solid tumors are often less apparent and difficult to demonstrate, likely due to the rigid structures of the carriers, which may prevent penetration to deeper regions within tumor tissue. Herein, we developed a flexible nanocarrier (FNC) system that is able to penetrate to deeper regions within tumor tissue. Specifically, we employed previously found flexible polyplexes comprised of siRNA and poly-L-lysine as wick structures for the preparation of FNCs. FNCs were constructed by coating the wick structures with lipids using a liposomal membrane fusion method. The diameters of the resulting FNCs were ca. 170 nm, and the shapes were non-spherical. Lipid coating was confirmed using a nuclease resistance assay. Furthermore, FNCs showed significant RNA interference effects, comparable to Lipofectamine 2000, in a mono-layered cell system. To accelerate tumor penetration, the FNC surface was modified with polyethylene glycol (PEG) and the tight junction opener peptide AT1002. Surface-modified FNCs demonstrated effective penetrability into a cancer spheroid. Thus, we developed a novel and unique tumor-penetrable siRNA FNC system.

Keywords: flexible nanocarrier; intercellular penetrability; siRNA/PLL polyplexes

Introduction

Small interfering RNA (siRNA) is expected to become a novel and effective nucleic acid medicine for cancer therapy (Boccellino, 2015; Kim, 2016). Effective anti-cancer therapeutic applications, however, require delivery of siRNA to the tumor site. Various non-viral delivery systems, such as polyplexes and lipoplexes, have been developed to deliver siRNA to tumor sites (Ballarín-González, 2014; Ozpolat, 2014; Zhang, 2014; Kim, 2016). In general, such delivery systems are typically spherical nanoparticles comprised of tightly condensed core structures that are formed via electrostatic interactions (Akita, 2010; Ballarín-González, 2014). Effective anti-cancer therapeutic carriers need to be able to penetrate into deep regions of tumor tissue through the narrow gaps that exist between cancer cells. Moreover, the rigid structures of such carriers are disadvantageous for deep penetration into tumor tissue through the intercellular space. In fact, penetration capability of nanoparticles depends on size. Kataoka's group found that 30 nm nanoparticles efficiently penetrated into tumor tissue, although penetration of 70 nm nanoparticles was not effective (Nishiyama 2016). Thus, smaller size would be suitable for penetration through the narrow gaps among cancer cells. In addition, nanoparticles modified with functional devices, such as cyclic tumor homing peptide, showed high permeability into tumor (Song 2016). Furthermore, it has been reported that ultra-formable liposomes, which have

high flexibility, have high permeability into skin tissues (Subongkot 2014). Therefore, it was suggested that the more flexible carrier structures would be required for penetration into tumor.

Previously, we found that polyplexes comprised of siRNA and poly-L-lysine (PLL) were able to pass through acrylamide gel, while other polyplexes of siRNA condensed with stearyl-octaarginine or protamine were unable to migrate in the gel (Nakamura, 2007). These results suggest that siRNA/PLL polyplexes form flexible structures that allow for penetration through narrow spaces in acrylamide gel, and that such structures may also be expected to penetrate through narrow intercellular gaps. As siRNA is known to be sensitive to nuclease activity, lipid coating of the flexible polyplexes is required for protection against nuclease attack, so we attempted to design a novel siRNA carrier comprised of a lipid-coated flexible siRNA/PLL polyplex.

Specifically, in the present study, we prepared wick structures comprised of siRNA and PLL, and constructed flexible nanocarriers (FNCs) by coating the wick structures with lipid membranes as shown in Figure 1. A previously developed liposomal membrane fusion method was employed to coat the polyplexes with a lipid bilayer to prepare a multifunctional envelope nano-device (MEND) (Nakamura, 2006; Akita, 2010). The functionality of the resulting FNCs was evaluated, including RNA interference (RNAi) effects and penetrability. Furthermore, based

on the results of the penetration study, the FNC surface was modified with functional devices to allow for accelerated penetrability.

Materials and Methods

Materials

Poly-L-lysine (PLL) (MW 23,900) was purchased from Sigma-Aldrich, Inc. (St. Louis, MO, USA). Alexa 546-labeled siRNA (21-mer, 5'-Alexa546-UAUUGCGUCUGUACACUCUCATT-3', 5'-Alexa546-UGAGUGUACAGACGCAAUATT-3') and anti-luciferase siRNA (21-mer, 5'-GCGCUGCUGGUGCCAACCCTT-3', 5'-GGGUUGGCACCAGCAGCGCTT-3') were obtained from Invitrogen Life Technologies (Carlsbad, CA, USA). 1,2-dioleoyl-3-trimethylammonium-propane (DOTAP), 1,2-dioleoyl-sn-glycero-3-phosphoethanolamine (DOPE) and 7-nitrobanz-2-oxa-1,3-diazole-DOPE (NBD-DOPE) were purchased from Avanti Polar Lipids (Alabaster, AL, USA). N-(carbonyl-methoxypolyethyleneglycol 2000)-1,2-distearoyl-sn-glycero-3-phosphoethanolamine (PEG_{2000}-DSPE) was purchased from the NOF Corporation (Tokyo, Japan). Lipofectamine 2000 (LFN) was obtained from Invitrogen Life Technologies (Carlsbad, CA, USA). Stearylated AT1002 (Stearyl-Phe-Cys-Ile-Gly-Arg-Leu-NH_2) was synthesized by Scrum Inc. (Tokyo, Japan). The mouse melanoma cell line B16-F1 was obtained from Dainippon Sumitomo Pharma Biomedical Co, Ltd. (Osaka, Japan), and stable transformants of B16-F1 cells expressing luciferase

(B16-F1-Luc) were established in our laboratory (Hama, 2012a). These cells were cultivated in DMEM supplemented with 10% FBS at 37°C in 5% CO_2.

Construction of flexible nanocarriers (FNCs)

A schematic of the FNC construction process is shown in Figure 1. The FNC construction process consists of two steps: (1) siRNA solution is mixed with poly-L-lysine solution to form a negatively charged wick structure via electrostatic interactions, and (2) cationic liposomes comprised of DOTAP/DOPE (1:1) are added to the wick structure suspension. The cationic liposomes associate with the surfaces of the negatively charged wick structures, and the wick structures are then coated with lipid membranes via membrane fusion between liposomes containing the membrane-fusible lipid DOPE, resulting in the formation of FNCs.

Wick structures were prepared by gently mixing a drop of siRNA solution (0.05 mg/ml) with a drop of PLL solution (0.1 mg/ml), and allowing the mixture to incubate for 10 min at room temperature. The cationic liposomes were prepared using a lipid hydration method (Hama 2012b, 2012c). Chloroform solution containing 0.1 μmol DOTAP and 0.1 μmol DOPE was dried to a thin film under vacuum in a test tube. The dried lipid film was hydrated with 0.4 mL 10 mM Tris buffer (pH 7.4) at room temperature to obtain a liposomal suspension, and

liposomes were produced by sonication in a bath-type sonicator (AU-25C, Aiwa, Tokyo, Japan). To modify the FNC surface, a solution of stearylated AT1002 and/or PEG-DSPE was added to the FNC suspension, and the mixture was incubated for 30 min at room temperature. Amounts of stearylated AT1002 and PEG-DSPE were 5 mol% and 1 mol% of total lipids, respectively. The diameters and zeta-potentials of the resulting wick structures, liposomes and FNCs were measured by dynamic light scattering and laser Doppler using a Zetasizer nano (Malvern Instruments Ltd, UK).

Native polyacrylamide gel electrophoresis of siRNA

Solutions of siRNA (20 pmol) mixed with PLL solution at various nitrogen/phosphate (N/P) ratios were subjected to native polyacrylamide gel electrophoresis using 15% polyacrylamide gel at 10.5 mA for 30 min. Following electrophoresis, the gel was stained with SYBR Gold solution (Invitrogen Life Technologies, Carlsbad, CA, USA) for 30 min, and the gel was observed under a UV transilluminator.

Ethidium bromide (EtBr) exclusion assay of wick structures prepared at various N/P ratios

A solution containing 0.1 μg EtBr was added to the suspension of wick structures containing 0.25 μg siRNA for intercalation of EtBr into siRNA. The fluorescence intensity of

EtBr intercalated in siRNA was then measured at an excitation wavelength of 260 nm and an emission wavelength of 630 nm (Sutton, 2006).

Sucrose density gradient fractionation analysis of FNCs

Labeling of both the siRNA and FNC lipid membrane was carried out by mixing a siRNA solution containing 10% Alexa546-labeled siRNA and a lipid mixture containing 1% NBD-DOPE. The labeled FNC sample was then applied to a discontinuous sucrose density gradient (0 - 60%), and ultracentrifugation was performed at 220,000 × *g* for 2 h at 20°C. After ultracentrifugation, 1 mL of solution was collected at a time. Fluorescence intensities of both Alexa and NBD in each fraction were measured at an excitation 546 nm/emission 573 nm and excitation 459 nm/emission 534 nm, respectively.

RNase protection assay

An RNase protection assay was performed according to our previous report (Yamada, 2016). Briefly, the FNC sample was incubated in the presence of RNase (10 μg/ml) for 2 h at 37°C. The sample was then solubilized with detergent on ice, and subjected to electrophoresis using 2% agarose gel at 100 V for 20 min. After electrophoresis, the gel was stained with SYBR Gold solution for 30 min, and observed under a UV transilluminator.

Negative staining and transmission electron microscopic observation of FNCs

The samples were absorbed to formvar film coated copper grids (400 mesh) and stained with 2% phosphor tungstic acid solution (pH 7.0) for 1 min. The samples were then observed using a transmission electron microscope (TEM) (JEM-1400Plus; JEOL Ltd., Tokyo, Japan) at an acceleration voltage of 80 kV. Digital images (2048 × 2048 pixels) were taken with a CCD camera (VELETA; Olympus Soft Imaging Solutions GmbH, Münster, Germany).

Transfection of FNCs containing anti-luciferase siRNA to cultured cells stably expressing luciferase

B16-F1 cells stably expressing luciferase were seeded on a culture well (4×10^4 cells/well). After 24 h, samples containing 15 pmol siRNA (60 nM) were added to the cultured cells and incubated for 48 h at 37°C. The cells were then solubilized with reporter lysis buffer. Luciferase activity of the cell lysate was measured as chemiluminescence intensity using a luminometer in the presence of luciferase assay reagent (Promega, Madison, WI, USA). The chemiluminescence intensity was compensated by protein amount evaluated with the BCA Protein Assay Kit (Thermo Fisher Scientific Inc., Waltham, MA, USA).

Penetrability of FNC into a cancer cell spheroid

To prepare the spheroid, a suspension of B16-F1 cells (3×10^4 cells) was added to a well of a NanoCulture Plate (Scivax, Kawasaki, Japan). After 1 day, a lump of cells was transferred to a glass-bottom dish coated with PLL, and incubated for 3 days. FNCs comprised of Alexa 546-labeled siRNA and NBD-labeled lipid membranes were prepared for observation with a confocal laser scanning microscope. The FNC suspension containing 100 nM siRNA was added to the cell spheroid, and incubated for 24 h. After incubation, 10 μL of 2.5 mM Hechest33342 was added, and the spheroid was incubated for 10 min at room temperature. The spheroid was then washed with DMEM without serum, and observed with a confocal laser scanning microscope (Nikon A1R, Nikon Tokyo).

Statistical analysis

Statistical analysis was performed using one-way ANOVA followed by Turkey-Kramer honest significant difference (HSD) test. P values <0.05 were considered to be significant; they were evaluated using JMP software (SAS Institute Inc. Cary, North Carolina, USA).

Results and Discussion

Preparation of wick structures comprised of siRNA and PLL

In our previous study, complexes of siRNA with PLL were prepared at an N/P ratio of 2.4, and were shown to penetrate through an acrylamide gel (Nakamura, 2007). In this study, we prepared siRNA/PLL complexes at various N/P ratios in an effort to find optimum condition for preparation of flexible wick structures of FNC. Complexes prepared at an N/P ratio 0.2 resulted in the appearance of novel bands at around 200 bp, while only one band attributed to siRNA was observed for complexes prepared at an N/P ratio of 0.1 (Figure 2). The intensities of the higher bands around 200 bp were found to increase with increasing N/P ratios. In contrast, no bands were observed at 200 bp for complexes prepared using an N/P ratio of 3.2 (Figure 2), indicating that the complexes prepared at this N/P ratio could not penetrate into the acrylamide gel. In Figure 2, two apparent bands around 200 bp were recognized. Thus, two fractions of wick structure would be formed by mixing of siRNA with PLL. Different numbers of siRNA would bind with PLL, although it is difficult to estimate the exact number of siRNA binding with PLL. The size and surface charges of a series of wick complexes prepared at N/P from 0.1 to 3.2 were measured (Supplemental table 1). Diameters of all complexes were over 150 nm. At N/P ratio 3.2, zeta-potential of the complex was positive, although the complexes prepared at lower N/P ratios showed negative zeta-potential. The size and surface charge of complexes were

not same. However, migrations of wick complexes prepared at all N/P ratios in gel electrophoresis were almost the same. Thus, the migration of complexes would not be affected by the size and surface charge in this study.

To precisely evaluate the formation of complexes comprised of siRNA and PLL, an EtBr exclusion assay was performed. Since EtBr can intercalate into double stranded nucleic acids (Sutton, 2006), the fluorescence intensity of EtBr can be used as an indicator of the formation of typical complexes, which would have tight structure. As shown in Figure 3, EtBr fluorescence exhibited similar intensities for complexes prepared at N/P ratios <1.0, while EtBr fluorescence decreased for complexes prepared at N/P ratios >1.0. These results suggest that typical complexes are prepared using N/P ratios >1.0. Thus, a fixed N/P ratio of 0.8 was used for the preparation of siRNA/PLL complexes to serve as wick structures to subsequently prepare FNCs. Diameters and zeta-potentials of the resulting wick structures were ca. 293 nm and -13 mV, respectively (Table 1).

Construction of FNCs by the liposomal membrane fusion method

To protect siRNA from nuclease activity, wick structures were coated with lipid membranes. We previously developed a lipid coating method via membrane fusion of liposomes to construct a spherical gene delivery system coated with two lipid membranes (Nakamura,

2006; Akita 2010). As liposomal membrane fusion was also expected to be suitable for coating the wick structures, we applied the same liposomal membrane fusion method to prepare the FNCs in this study.

When positively charged liposomes containing the membrane-fusible lipid DOPE (with diameters and zeta-potentials ca. 130 nm and 27 mV, respectively [Table 1]) were added to the wick structure suspension, the liposomes easily fused with each other upon binding to the negatively charged surfaces of the wick structures via electrostatic interactions. After mixing the wick structure suspension with liposomes, the diameters and zeta-potentials of the resulting sample were ca. 170 nm and 23 mV, respectively (Table 1). The negative surface charge of the wick structures was inverted to positive upon mixing with liposomes. The sample was then subjected to density gradient ultracentrifugation fractionation analysis (Fig. 4). Significant amounts of lipid were detected in fractions #1 and #2, indicating that empty liposomes exist in those low-density fractions. On the other hand, only siRNA was recognized in fractions #11 and #12, suggesting that these fractions only contained wick structures. Fractions #4 - #6 were found to contain siRNA co-localized with lipid, suggesting that the lipid-coated wick structures, *i.e.*, FNCs, were contained in those fractions. The percentage of siRNA encapsulated into FNC was calculated from the result of density gradient ultracentrifugation fractionation analysis (Figure 4). The encapsulation percentage of siRNA in FNC was 51 %.

An RNase protection assay was carried out to confirm lipid coating of the wick structures (Fig. 5). In the absence of RNase, two bands were observed in the wick structure sample, namely a lower band corresponding to free siRNA, and an upper band corresponding to the wick structures (Fig. 5). When both free siRNA and the wick structures were treated with RNase, bands corresponding to siRNA disappeared, suggesting that the RNasse degraded the siRNA (Fig. 5). In the case of FNCs, an upper band was recognized even in the presence of RNase, while the lower band was found to disappear in the presence of RNase (Fig. 5). Taken together, these results suggest that only free siRNA, without a lipid coating, was degraded by RNase, and that FNCs were successfully constructed via lipid coating of the wick structures.

TEM was employed to examine the morphological structures of the resulting FNCs (Fig. 6). The shapes of the FNCs were found to be non-spherical, as evidenced by the elliptic particle shown in Fig. 6. Moreover, both lipid envelope structures and cavity spaces were recognized in the FNCs. In other images, similar non-spherical structures were also observed. In broader scope images of Supplemental figure 1, only one FNC was observed in the broader images because of low number of the nanoparticles in the diluted sample suspensions for TEM observation. In the broader images, small particles, which would be liposomes, were also observed. Based on the TEM images, the resulting shapes of the FNCs were different from those of more conventional delivery systems, such as lipoplexes and polyplexes. To clarify the reason

for non-spherical structure of FNC, the siRNA/PLL complexes were observed by AFM. As shown in the Supplemental figure 2, shape of siRNA/PLL complex was not a sphere, like a rod. Thus, the non-spherical structure of FNC would depend on the wick structure (siRNA/PLL complex).

Regarding flexibility of FNC, we additionally performed the observation of FNC by atomic force microscope (AFM). As shown in AFM image (Supplemental figure 3), height of FNC was less 50 nm, although diameter was over 300 nm. On the other hand, diameter measured by DLS was approximately 170 nm (Table 1). From these results, it was suggested that the nanoparticles were flattened in the AFM image. Thus, FNC should be flexible structure, although siRNA/PLL complexes were encapsulated in the nanoparticles.

Inhibitory effects of anti-luciferase siRNA-containing FNCs on luciferase activity of cultured cells

To confirm the functionality of FNCs for potential use as siRNA carriers, transfection of anti-luciferase siRNA-containing FNCs was examined in cells stably expressing luciferase cultured on a plane surface, and compared with siRNA lipoplexes comprised of the conventional transfection reagent Lipofectamine 2000 (LFN/siRNA) (Fig. 7). The anti-luciferase activity of FNC encapsulating anti-luciferase siRNA was examined against plane

culture cells stably expressing luciferase, not spheroid. We previously examined the effect of FNCs encapsulating anti-luciferase siRNA on spheroid expressing luciferase. However, since FNCs were taken up by the cells not only inside but also outside of spheroid, it was difficult to evaluate RNAi effect by penetration of FNCs into inside of spheroid. Thus, we used plane culture cells for evaluation of gene knockdown capability of FNCs. As shown, both LFN/siRNA lipoplexes and FNCs significantly reduced luciferase activity in the mono-layered cells, suggesting that the RNAi effect of the latter was comparable to that of LFN/siRNA lipoplexes. As shown in the Supplemental figure 4, FNCs encapsulating anti-GFP siRNA showed no inhibition of luciferase activity. This result indicates that non-specific knockdown effect on luciferase activity was not recognized in this study. Thus, it was confirmed that reductions of luciferase activity in Figures 7 and 9 were specific RNAi effect of FNCs encapsulating anti-luciferase siRNA. Thus, FNC exhibits sufficient functionality as a siRNA carrier.

Penetrability of FNCs into cancer cell spheroid through intercellular space

To evaluate penetrability into a cancer cell spheroid, FNCs comprised of Alexa546-labeled siRNA (red)/PLL wick structures and NBD-labeled lipid membranes were prepared. FNCs labeled with fluorescent dyes were then incubated with the cancer spheroid, and the penetrability of FNCs into the spheroid was evaluated using a confocal laser scanning

microscope (Fig. 8). Minimal red fluorescence (siRNA) was recognized in a lump of cells; however, FNC penetration into the spheroid was not sufficient. To improve the penetrability, the FNC surface was modified with functional moieties. Based on previous reports, we selected AT1002 as a functional peptide moiety to allow for penetration through the intercellular space. AT1002 is a synthetic peptide comprised of six amino acids (Phe-Cys-Ile-Gly-Arg-Leu-Cys-Gly) known to induce reversible opening of tight junctions by changing the zonula occludens protein 1 (ZO-1), like Zonula occuluta toxin (Zot) (Song, 2008a, 2008b). Previously, the Okada group reported that transdermal penetration of siRNA complexes was enhanced by co-application with AT1002 (Uchida, 2011a, 2011b). In this study, the FNC surface was modified by incubation with AT1002 conjugated with stearic acid. Modification with AT1002 (5 mol % of total lipids) did not change significantly the diameters or zeta-potentials of the FNCs (Table 1). However, the zeta-potential of FNCs was slightly decreased by modification with AT1002 or PEG, although the decrease in the zeta-potential was not statistically significant. Based on this result, it was suggested that AT1002 or PEG was loaded on the surface of FNCs.

When AT1002-modified FNCs (AT1002-FNCs) were incubated with the spheroid, a potent red fluorescence signal was observed in the peripheral region of the spheroid, indicating aggregation of AT1002-FNC on the spheroid surface (Fig. 8). It is likely that the hydrophobic

amino acid residues (Phe, Ile and Leu) of the AT1002 peptide are responsible for the observed FNC aggregation. To prevent aggregation on the peripheral regions of the spheroid, the FNC surface was modified with polyethylene-glycol (PEG). No significant changes in zeta-potentials were observed upon modification with PEG (1 mol% of total lipids), while the diameters of the PEG-modified FNCs (PEG-FNCs) were slightly smaller than those of non-modified FNCs (Table 1). The PEG-FNCs were then incubated with the spheroid. Since red fluorescence of the PEG-FNCs was observed mainly on the surface of spheroid, it was suggested that the PEG-FNCs could not penetrate into the spheroid, despite the fact that aggregation should have been somewhat prevented by modification with PEG.

FNCs equipped with both functional devices, namely AT1002 for intercellular penetration, and PEG for prevention of aggregation, were subsequently prepared. Physicochemical properties of the FNCs modified with both AT1002 and PEG (AT1002/PEG-FNCs) were nearly identical to those of PEG-FNCs (Table 1). Incubation of the AT1002/PEG-FNCs with the spheroid resulted in homogenously distributed red fluorescence throughout the spheroid, although some small amounts of aggregation were also observed (Fig. 8). Based on these findings, it is suggested that the AT1002/PEG-FNCs exhibit the ability to penetrate into the narrow intercellular spaces of the spheroid. Thus, AT1002 and PEG represent a suitable combination for effective penetration into cellular clumps. Regarding spheroid

experiment, it would be ideal that spheroid structures are almost the same for better evaluation. In this study, we used mouse melanoma B16-F1 cells as cancer cells, and prepared spheroid of this melanoma cells, because we established B16-F1 cells stably expressing luciferase. However, the spheroid of B16-F1 cells was fragile. Thus, when the spherical spheroid was transferred from NanoCulture Plate to a glass-bottom dish, the shape was changed. In this study, FNC was not purified after mixing the wick complexes with liposomes. In our previous study, we developed novel liposomal-type gene delivery system octa-arginine modified multifunctional envelope-type nano device (R8-MEND) (Kogure 2007), and examined the effect of purification of R8-MEND encapsulating luciferase plasmid DNA on transfection activity. The luciferase activity of purified R8-MEND was lower than that of un-purified R8-MEND (Unpublished data). It was suggested that the empty R8-modified liposomes, which co-existed with R8-MEND in the suspension, were necessary for high functionality of the gene delivery nanoparticles. Thus, in this study, we did not purify FNCs. Probably, AT1002/PEG-modified liposomes, which co-existed with AT-1002/PEG-FNCs in the suspension, also contribute for opening intercellular junction.

Since the FNCs were constructed as siRNA carriers, the knockdown activity of FNCs against specific gene expression should be maintained even after surface modification with AT1002 and PEG. To confirm this, transfections of FNCs containing anti-luciferase siRNA

modified with AT1002 and/or PEG were examined against B16-F1 cells stably expressing luciferase. The suppression activities of FNCs modified with AT1002, PEG and AT1002/PEG were nearly the same, and no statistical significant differences between non-modified and modified FNCs were observed, although the activity of non-modified FNCs was slightly decreased by modification (Fig. 9). These results indicate that surface modification with AT1002 and/or PEG did not prevent the ability of FNCs to function as siRNA carriers.

Regarding the surface modifications, PEG should also be useful for blood circulation to deliver FNCs to tumor tissue by the enhanced permeability and retention (EPR) effect. However, the PEG-to-AT1002 ratio should be optimized for such *in vivo* applications. It is currently difficult to optimize the PEG-to-AT1002 ratio for both protracted blood circulation and intercellular penetration using an *in vivo* tumor bearing animal model. In the future, however, such optimizations will be required for *in vivo* applications of AT1002/PEG-FNCs for cancer therapy.

Conclusion

In this study, flexible nanocarriers (FNCs) were developed that exhibit the ability to penetrate tumor tissue through the intercellular space. For effective intercellular penetration, the FNC surface was modified with the tight junction opener peptide AT1002. FNCs were further

modified with PEG for prevention of AT1002-mediated aggregation of FNCs on the surface of the cancer spheroid. The surface-modified FNCs were found to effectively penetrate into the cancer spheroid without any reduction in their ability to serve as siRNA carriers. In conclusion, a novel intercellular penetrable siRNA carrier was successfully developed based on a unique concept.

Acknowledgements

This work was partly supported financially in part by a grant from the Ministry of Education, Culture, Sports, Science and Technology of Japan (MEXT)-Supported Program for the Strategic Research Foundation at Private Universities, 2013-2017 (S1311035), and JSPS KAKENHI Grant Numbers 15K14945.

References

Akita H., Kogure K., Moriguchi R., Nakamura Y., Higashi T., Nakamura T., Serada S., Fujimoto M., Naka T., Futaki S., Harashima H., 2010. Nanoparticles for ex vivo siRNA delivery to dendritic cells for cancer vaccines: programmed endosomal escape and dissociation. J. Control. Release 143, 311-317.

Ballarín-González B., Ebbesen M.F., Howard K.A., 2014. Polycation-based nanoparticles for RNAi-mediated cancer treatment. Cancer Lett. 352, 66-80.

Boccellino M., Alaia C., Misso G., Cossu A.M., Facchini G., Piscitelli R., Quagliuolo L., Caraglia M., 2015. Gene interference strategies as a new tool for the treatment of prostate cancer. Endocrine. 49, 588-605.

Hama S., Utsumi S., Fukuda Y., Nakayama K., Okamura Y., Tsuchiya H., Fukuzawa K., Harashima H., Kogure K., 2012a. Development of a novel drug delivery system consisting of an antitumor agent tocopheryl succinate. J. Control. Release 161, 843-851.

Hama S., Uenishi S., Yamada A., Ohgita T., Tsuchiya H., Yamashita E., Kogure K., 2012b. Scavenging of hydroxyl radicals in aqueous solution by astaxanthin encapsulated in liposomes. Biol Pharm Bull. 35, 2238-2242.

Hama S., Takahashi K., Inai Y., Shiota K., Sakamoto R., Yamada A., Tsuchiya H., Kanamura K., Yamashita E., Kogure K., 2012c. Protective effects of topical application of a poorly

soluble antioxidant astaxanthin liposomal formulation on ultraviolet-induced skin damage. J. Pharm. Sci. 101, 2909-2916.

Kim H.J., Kim A., Miyata K., Kataoka K., 2016. Recent progress in development of siRNA delivery vehicles for cancer therapy. Adv. Drug Deliv. Rev. 104, 61-77.

Kogure K., Akita H., Harashima H., 2007. Multifunctional envelope-type nano device for non-viral gene delivery: concept and application of Programmed Packaging. J Control Release. 122, 246-251.

Nakamura T., Moriguchi R., Kogure K., Minoura A., Masuda T., Akita H., Kato K., Hamada H., Ueno M., Futaki S., Harashima H., 2006. Delivery of condensed DNA by liposomal non-viral gene delivery system into nucleus of dendritic cells. Biol Pharm Bull. 29, 1290-1293.

Nakamura Y., Kogure K., Futaki S., Harashima H., 2007. Octaarginine-modified multifunctional envelope-type nano device for siRNA. J. Control. Release 119, 360-367.

Nishiyama N., Matsumura Y., Kataoka K., 2016. Development of polymeric micelles for targeting intractable cancers. Cancer Sci. 107, 867-874.

Ozpolat B., Sood A.K., Lopez-Berestein G., 2014. Liposomal siRNA nanocarriers for cancer therapy. Adv. Drug Deliv. Rev. 66, 110-116.

Song K.H., Fasano A., Eddington N.D., 2008a. Effect of the six-mer synthetic peptide (AT1002) fragment of zonula occludens toxin on the intestinal absorption of cyclosporin A. Int. J. Pharm. 351, 8-14.

Song K.H., Fasano A., Eddington N.D., 2008b. Enhanced nasal absorption of hydrophilic markers after dosing with AT1002, a tight junction modulator. Eur. J. Pharm. Biopharm. 69, 231-237.

Song X., Wan Z., Chen T., Fu Y., Jiang K., Yi X., Ke H., Dong J., Yang L., Li L., Sun X., Gong T., Zhang Z., 2016. Development of a multi-target peptide for potentiating chemotherapy by modulating tumor microenvironment. Biomaterials. 108, 44-56.

Subongkot T., Pamornpathomkul B., Rojanarata T., Opanasopit P., Ngawhirunpat T., 2014. Investigation of the mechanism of enhanced skin penetration by ultradeformable liposomes. Int J Nanomedicine. 9, 3539-3550.

Sutton D., Kim S., Shuai X., Leskov K., Marques J.T., Williams B.R., Boothman D.A., Gao J., 2006. Efficient suppression of secretory clusterin levels by polymer-siRNA nanocomplexes enhances ionizing radiation lethality in human MCF-7 breast cancer cells in vitro. Int J Nanomedicine. 1, 155-162.

Uchida T., Kanazawa T., Takashima Y., Okada H., 2011a. Development of an efficient transdermal delivery system of small interfering RNA using functional peptides, Tat and AT-1002. Chem. Pharm. Bull. 59, 196-201.

Uchida T., Kanazawa T., Kawai M., Takashima Y., Okada H., 2011b, Therapeutic effects on atopic dermatitis by anti-RelA short interfering RNA combined with functional peptides Tat and AT1002. J. Pharmacol. Exp. Ther. 338, 443-450.

Yamada A., Mitsueda A., Hasan M., Ueda M., Hama S., Warashina S., Nakamura T., Harashima H., Kogure K., 2016. Tri-membrane nanoparticles produced by combining liposome fusion and a novel patchwork of bicelles to overcome endosomal and nuclear membrane barriers to cargo delivery. Biomater. Sci. 4, 439-447.

Zhang J., Li X., Huang L., 2014. Non-viral nanocarriers for siRNA delivery in breast cancer. J. Control. Release 190, 440-450.

Table 1. Characteristics of the various structures prepared in this study

Sample	Diameter (nm)	Poly dispersion index	Zeta-potential (mV)
Wick structures	293.1±76.7	0.35±0.12	-13.3±3.1
Liposomes	127.4 ± 28.9	0.34 ± 0.07	26.5 ± 5.1
FNCs	168.1 ± 27.9	0.26 ± 0.06	22.9 ± 6.6
AT1002-FNCs	169.1 ± 25.9	0.28 ± 0.08	20.7 ± 5.3
PEG-FNCs	154.5 ± 33.0	0.23 ± 0.08	20.4 ± 8.9
AT1002/PEG-FNCs	151.8 ± 26.2	0.24 ± 0.06	20.8 ± 6.2

Values are means ± SD obtained by measurement of at least three different samples.

Figure legends

Figure 1.

Schematic of the process for construction of flexible nanocarriers (FNCs)

FNCs were constructed in two steps: (1) preparation of wick structures by mixing siRNA and poly-L-lysine, as poly-L-lysine and siRNA easily make a flexible complex via electrostatic interactions, and (2) lipid coating of wick structures. After addition of cationic liposomes to the wick structures, the liposomes associate on the surfaces of the wick structures via electrostatic interactions. As the liposomes contain the membrane-fusible lipid DOPE, membrane fusion among the liposomes occurs and the wick structures are covered with two lipid membranes.

Figure 2.

Polyacrylamide gel electrophoresis of siRNA after incubation with PLL at various N/P ratios

Samples prepared by mixing siRNA with PLL at various N/P ratios were subjected to polyacrylamide gel electrophoresis. The gel was stained with SYBR Gold and observed under UV light. The lower band corresponds to free siRNA, while the higher band is attributed to wick structures comprised of siRNA with PLL.

Figure 3.

Fluorescence intensity of EtBr intercalated in siRNA/PLL complexes prepared at various N/P ratios

Fluorescence intensity of EtBr was measured after addition of the dye with a suspension of siRNA/PLL complexes prepared at various N/P ratios. EtBr fluoresces upon intercalation into double stranded siRNA structures. Low fluorescence intensity is indicative of a tightly bound siRNA/PLL complex.

Figure 4.

Sucrose density gradient fractionation of FNCs

For sucrose density gradient fraction analysis, FNCs comprised of Alexa546-labeled siRNA and NBD-labeled lipid membranes were prepared. After sucrose density gradient fractionation of FNCs, fluorescence intensities of Alexa546-labeled siRNA (closed triangle) and NBD-labeled lipid (open square) in each fraction were measured at excitation 546 nm/emission 573 nm and excitation 459 nm/emission 534 nm, respectively.

Figure 5.

RNase protection assay of wick structures and FNCs

Samples were treated with RNase (10 μg/ml) for 2 h at 37°C, then subjected to agarose gel electrophoresis. After the electrophoresis, the gel was stained with SYBR Gold solution for 30 min, and observed under a UV transilluminator.

Figure 6.

TEM image of FNCs treated after negative staining

FNCs stained with phosphor tungstic acid were observed by TEM. The bar represents 100 nm.

Figure 7.

Effect of FNCs encapsulating anti-luciferase siRNA on luciferase activity

FNCs encapsulating anti-luciferase siRNA or Lipofectamine 2000/anti-luciferase siRNA complexes were transfected into B16-F1 cells stably expressing luciferase. After a 48 h incubation at 37°C, the luciferase activity was measured. Data are means ± SD obtained from 3 different samples. *$p < 0.05$, **$p < 0.01$.

Figure 8.

Confocal microscopy of the cancer spheroid after addition of various FNCs

A suspension of FNCs encapsulating Alexa546-labeled siRNA was added to the spheroid. After 24 h incubation at 37°C, cell nuclei of the spheroid were stained with Hechest33342 for 10 min. The spheroid was then observed with a confocal laser scanning microscope. Confocal images in the x-y plane at 54-60 μm distance (direction along the z-axis) from surface of 3D-cultured B16-F1 cells. Scale bars: 50 μm.

Figure 9

Effect of various FNCs encapsulating anti-luciferase siRNA on luciferase activity

Various FNCs encapsulating anti-luciferase siRNA were transfected into B16-F1 cells stably expressing luciferase. After a 48 h incubation at 37°C, the luciferase activity was measured. Suppression activity of the FNCs was obtained by dividing the decrease in luciferase activity by the luciferase activity of untreated cells. Data are means ± SD obtained from 3 different samples.

Figure 1

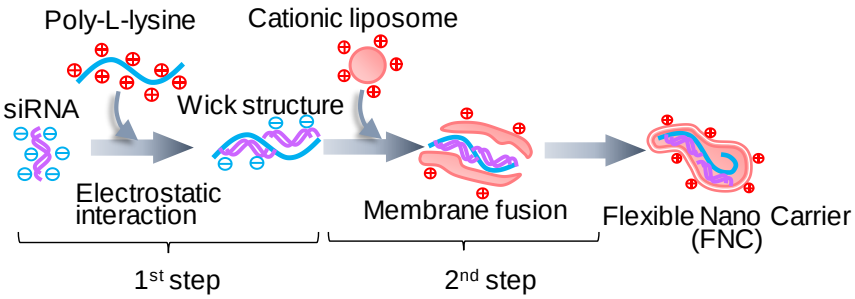

Figure 2

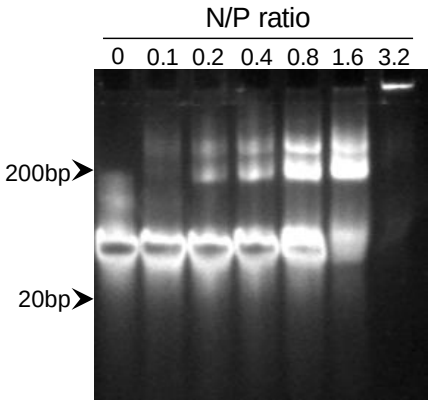

Figure 3

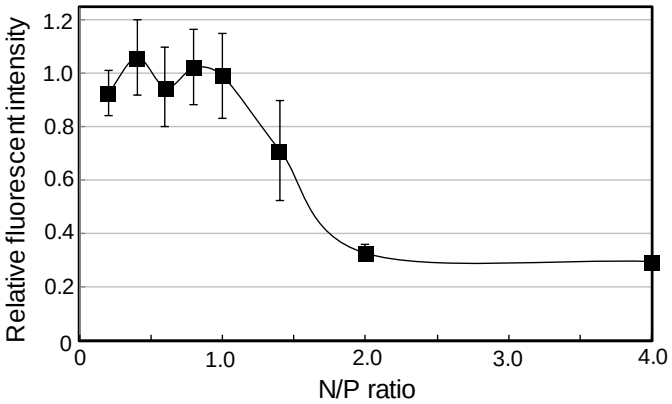

Figure 4

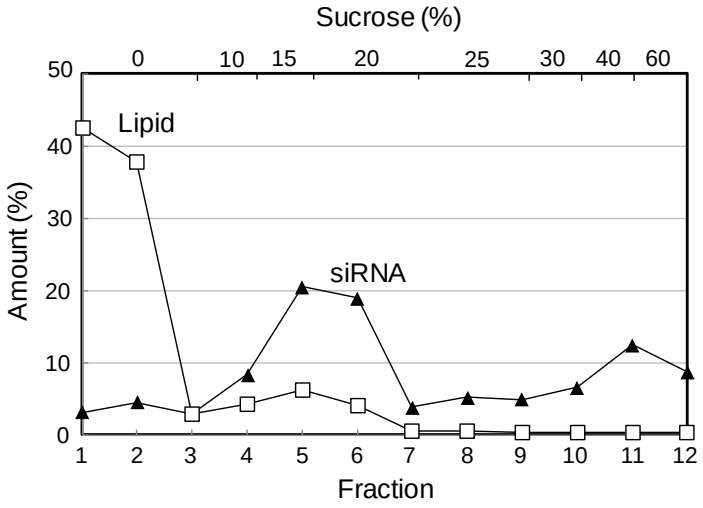

Figure 5

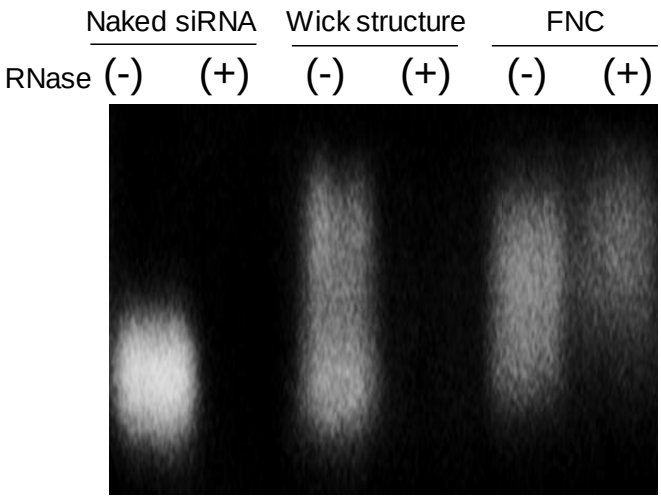

Figure 6

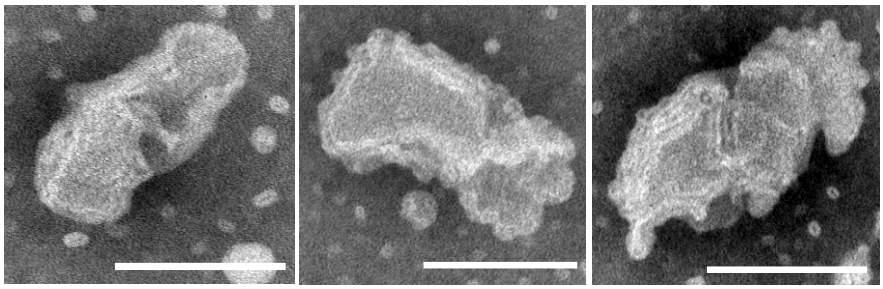

Figure 7

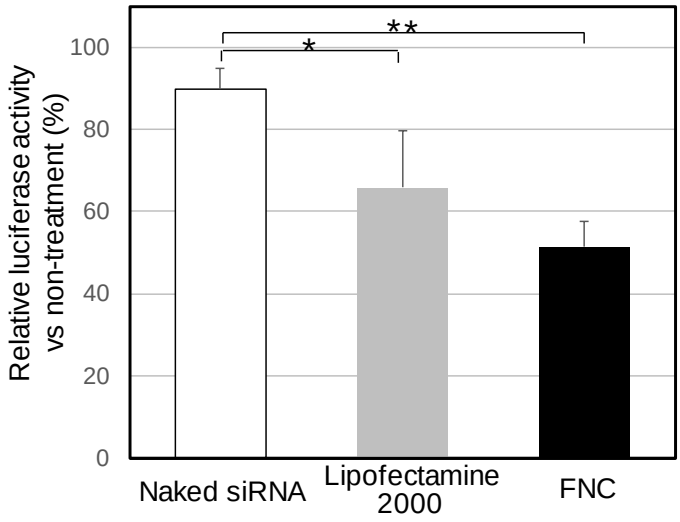

Figure 8

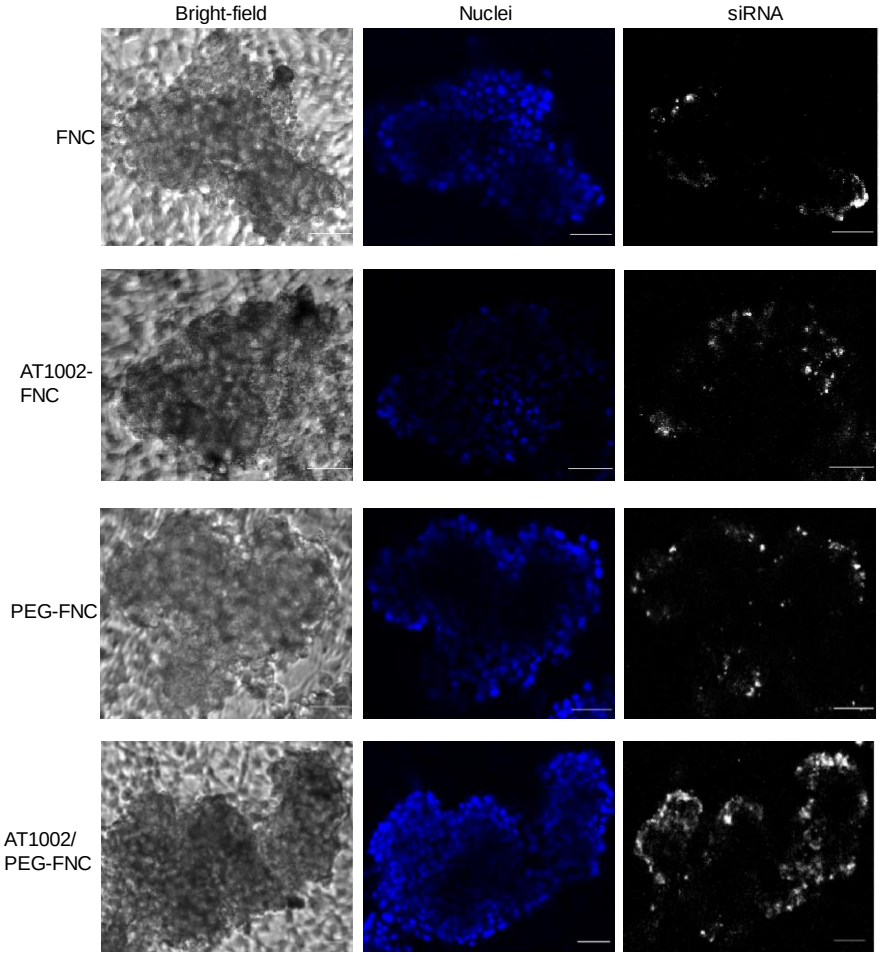

Figure 9

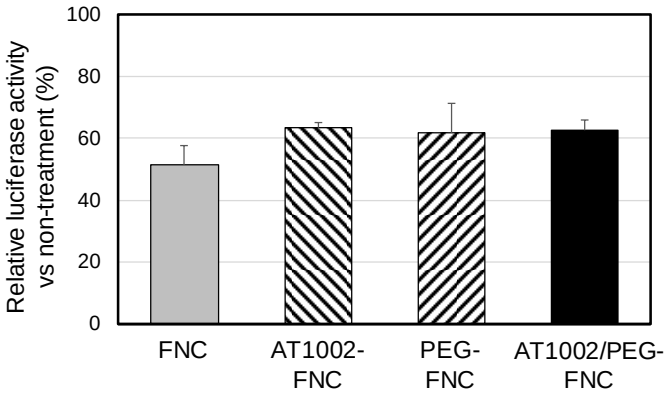

Supplemental table 1

Supplemental table 1. Characteristics of the siRNA/PLL complexes prepared at various N/P ratios

N/P ratio	Diameter (nm)	PDI	Zeta-potential (mV)
0.1	310.7 ± 52.0	0.75 ± 0.22	-5.6 ± 3.0
0.2	367.3 ± 156.4	0.76 ± 0.22	-6.8 ± 9.8
0.4	175.5 ± 46.1	0.84 ± 0.28	-10.9 ± 12.8
0.8	293.1 ± 76.7	0.35 ± 0.12	-13.3 ± 3.1
1.6	209.3 ± 105.5	0.41 ± 0.51	-0.5 ± 5.9
3.2	195.9 ± 24.8	0.18 ± 0.10	7.8 ± 5.4

Values are means ± SD obtained by measurement of at least three different samples.

Supplemental figure 1

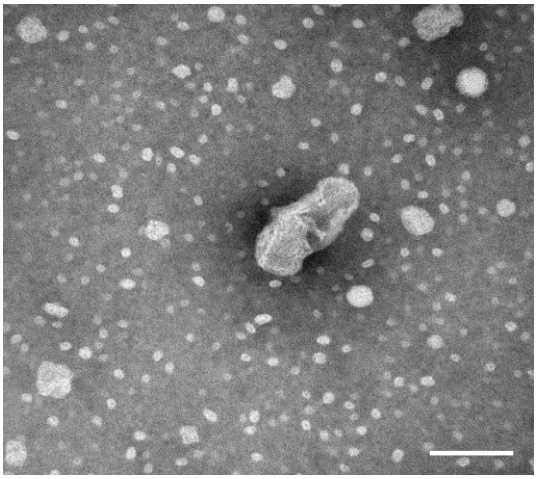

Supplemental figure 1. TEM image of FNCs with a broader scope treated after negative staining
FNCs stained with phosphor tungstic acid were observed by TEM. The bar represents 100 nm.

Supplemental figure 2

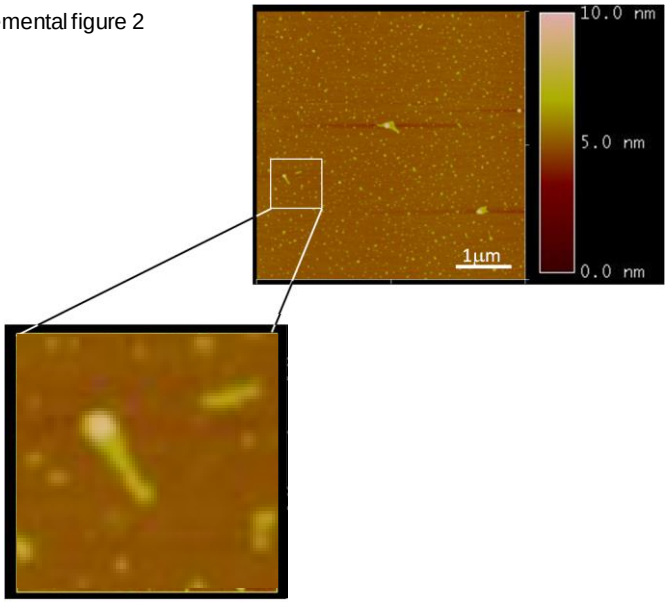

Supplemental figure 2. Atomic force microscope (AFM) image of siRNA/PLL complexes prepared at N/P=0.8
The sample diluted up to 10 times was dropped on freshly cleaved mica, then the mica was dried for two hours in the desiccator. After that, the sample was observed by tapping mode with AFM Nanoscope IIIa (Digital Instruments Inc. NY USA).

Supplemental figure 3

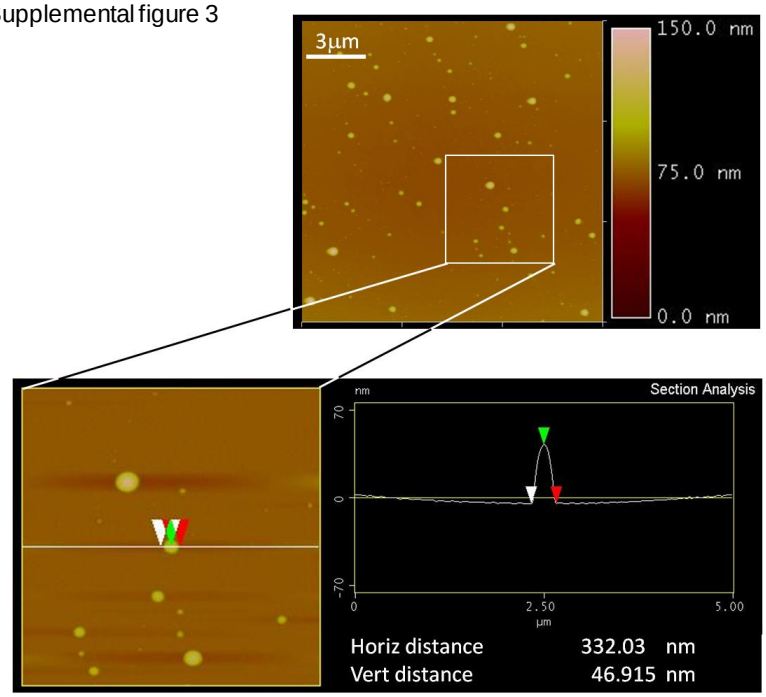

Supplemental figure 3. Atomic force microscope (AFM) image of FNC
The sample diluted up to 10 times was dropped on freshly cleaved mica, then the mica was dried for two hours in the desiccator. After that, the sample was observed by tapping mode with AFM Nanoscope IIIa (Digital Instruments Inc. NY USA).

Supplemental figure 4

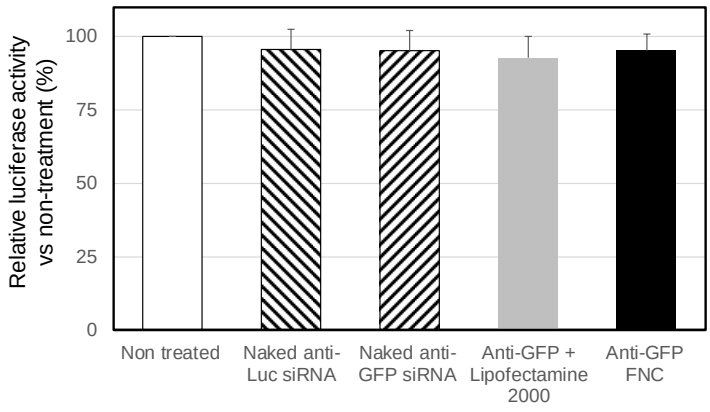

Supplemental figure 4. Effect of FNCs encapsulating anti-GFP siRNA on luciferase activity
FNCs encapsulating anti-GFP siRNA or Lipofectamine 2000/anti-GFP siRNA complexes were transfected into B16-F1 cells stably expressing luciferase. After a 48 h incubation at 37° C, the luciferase activity was measured. Data are means ± SD obtained from 3 different samples.